Journal of Molecular Structure 1222 (2020) 128928

Contents lists available at ScienceDirect

Journal of Molecular Structure

journal homepage: www.elsevier.com/locate/molstr

Interaction of N-succinyl diaminopimelate desuccinylase with orphenadrine and disulfiram

Manuel Terrazas-López[a], Naún Lobo-Galo[a], Luis Guadalupe Aguirre-Reyes[a], Ismael Bustos-Jaimes[b], Jorge Ángel Marcos-Víquez[b], Lilian González-Segura[c], Ángel Gabriel Díaz-Sánchez[a,1,*]

[a] Universidad Autónoma de Ciudad Juárez, Instituto de Ciencias Biomédicas, Departamento de Ciencias Químico Biológicas, Ciudad Juárez 32310, Chihuahua, México
[b] Universidad Nacional Autónoma de México, Facultad de Medicina, Departamento de Bioquímica, Ciudad Universitaria, Ciudad de México 04510, México
[c] Universidad Nacional Autónoma de México, Facultad de Química, Departamento de Bioquímica, Ciudad Universitaria, Ciudad de México 04510, México

ARTICLE INFO

Article history:
Received 11 April 2020
Revised 12 July 2020
Accepted 17 July 2020

Keywords:
DapE
Antimicrobial target
Inhibition
Anti-DapE
M20-peptidase

ABSTRACT

The emergence of multiresistant, often persistent, pathogenic bacteria emphasizes the need for a continuous identification of new pharmacological targets of enzymatic nature, and the development of selective inhibitors against them. Ubiquitously present in most bacteria, the enzyme metallohydrolase N-succinyl diaminopimelate desuccinylase (DapE) is required for the biosynthesis of *meso*-diaminopimelate (*m*DAP) and lysine, both essential components of bacterial peptidoglycan. DapE activity has been recognized as critical for bacterial growth; and thus, it is a potential pharmacological target. In order to develop effective inhibitors against DapE, understanding of structural and functional features of the enzyme must be used in the design, such as the interaction of its metal centers with ligands, as well as its effect on global protein conformational changes that seem to produce an induced fit after ligand binding. Here, we propose the potential application of currently approved drugs, used in different medical fields, orphenadrine and disulfiram, as possible inhibitory compounds against DapE, based on studies of equilibrium ligand binding, inhibition, thermal stability and molecular docking into *Enterococcus faecium* and *Escherichia coli* DapE enzyme homologs. Drugs were selected based on key structural features, including the presence of soft heteroatoms or π-bonds that are known to interact with DapE active site. Enzymes from selected bacteria were chosen based on the pattern of infection, persistence, and drug resistance as well to study an enzyme from the two Gram classification. Furthermore, the information presented here can further provide structural details about key interacting functional groups, which should be considered in the design and development of a new generation of antibiotics that can target the essential DapE enzyme.

1. Introduction

Emerging multiresistant bacterial pathogens, which often establish persistent infections, represent a major public health problem that requires the development of new classes of antibiotics which can overcame the mechanisms of bacterial resistances [1,2]. Among these infections, those caused by a group of bacteria called ESKAPE (*Enteroccocus faecium, Staphylococcus aureus, Klebsiella pneumoniae, Acitenobacter baumannii, Pseudomonas aeruginosa* and *Enterobacter sp.*) and also *Escherichia coli* are of special interest, since they are responsible for most multiresistant and hard-to treat intra-hospital infections [3–5]. Given that many of these bacteria can also evade host-immunoresponses, control of these antibiotic-resistant infections requires the identification of new differential macromolecular targets, whose blocking results in a lethal effect to the bacteria, under the premise that their chemical inhibition will produce selective harmful effects only to the prokaryotic cells [6–8]. However, and relevant to this last aspect, the design and development of new specific inhibitors against these newly identified targets, is not a trivial, inexpensive and rapid task. An alternative and widely used approach to accelerate this process of discovery without compromising safety, is the pharmacological re-purposing of FDA-approved –drugs, extensively administered for treatment of other pathologies, as potential antimicrobial chemotherapeutic agents.

* Corresponding author.
E-mail address: angel.diaz@uacj.mx (J.Á. Marcos-Víquez).
[1] Postal address: Instituto de Ciencias Biomédicas, Departamento de Ciencias Químico Biológicas, Universidad Autónoma de Ciudad Juárez, Ciudad Juárez, Chihuahua 32310, México.

https://doi.org/10.1016/j.molstruc.2020.128928
0022-2860/

Ligand docking in macromolecules and their subsequent validation *in vitro* offers a recognized and successful strategy in this regard [9–11]. Notably, DapE, is one of these other potential targets [12], since its activity is essential in most bacteria, both Gram negative, and Gram positive organisms, and deletion of the encoding gene has been found to be lethal or important in some bacteria [13,14]. DapE is a metallohydrolase that has been extensively studied [13,15–24]. It is dependent of two Zn^{2+}metal ions centers; but replacement of one of these by a Mn^{2+} results in a changes in the preference of the substrate, as well as the susceptibility for by captopril [25], a known anti-DapE drug [20,26,27]. The bacterial enzyme is a strict homodimer [28], since part of its catalytic machinery is provided by the oligomerization domain of the opposite subunit when it enters to the active site upon conformational changes induced by the substrate binding [16]. During a catalytic cycle, an oxyanion intermediate is formed in the enzyme, which needs stabilization by two positively charged groups, provided by an oxyanion hole. One of these groups is composed by metal center 2 (Zn^{2+}) and the other is the imidazole ring of His194 (numeration of *Haemophilus influenzae* DapE, HiDapE, hereafter used) located in the oligomerization domain of subunit B [16]. During the closure of the dimer, also a residue of Tyr (197) and two of Asn (244 and 245) enter into the active site and appear to stabilize the polar groups of the N-succinyl-diaminopimelate (NSDAP) substrate, together with strictly conserved charged amino acids (two Glu and two Arg residues), which stabilize the amino and carboxyl groups present in the substrate [16], both of which are charged at physiological pH. It has been proposed that all of these critical structural features must be taken into account for the selection or design of specific inhibitors. Conceivably, the ideal DapE ligands must possess (1) metal-binding groups (MBGs, which are soft Lewis bases) to interact with the metal centers, and (2) moieties that can interact with either charged, polar or π-bonds containing groups present in the active site cavity. Compounds with known anti-DapE properties are relatively polar or charged molecules, containing one or more MBGs that interact and block the metal centers [20,26,27]. Other known inhibitors have phenyl derivatives (3-mercapto-benzoic acid, phenylboronic acid, carboxy-phenylboronic acids, enapril, N- (benzyloxycarbonyl) hydroxylamine, N-phenylthiourea) [20] or indoline derivatives [27,29]; a common chemical characteristic that probably allows them to interact with the aromatic or histidine residues present in the active site. Most of these inhibitors were identified by means of screenings of compounds containing MBGs and using the structure of HiDapE-ZnZn enzyme as the target; finding thiols, carboxylic acids, boronic acids, phosphonates and hydroxymates [20]; and more recently indolines [27,29].

One of the most studied DapE inhibitors is captopril, a compound that has an MBG which contains a thiol that reacts with, and blocks, the metal centers of the Zn-Zn-enzyme [26]. This drug is commonly used for the treatment of blood pressure in patients with hypertension by inhibiting the angiotensin-converting enzyme [30]. Notably, this enzyme is also a Zn^{2+}-dependent protease that captopril blocks by forming a coordination bond to the metal center [31]. Captopril was initially identified as a potential DapE inhibitor from a virtual screening study and its anti-DapE properties were subsequently validated [20,26]. Other potential anti-DapE agents were identified by *in silico* approaches from a drug-like small molecule-screening library [32].

To provide more information on the molecular structure and properties of additional DapE inhibitors, here we performed a search for potential ligands, using *in silico* techniques and the drugs Zinc database. We carried out the selection of new compounds by those that possess sulfur atoms since they are soft Lewis bases or those that contain aromatic moieties that could interact with the π-bonds containing groups of the active site. In addition, and for safety reasons, we only included compounds currently used as therapeutic drugs, with a long clinical use without significant side effects. From all potential compounds, we selected disulfiram (DSF) and orphenadrine (ORPH), since they both meet these characteristics. We further investigated if ORPH and DSF possessed structural and complementary characteristics capable of binding to the active site of DapE homologs of *E. faecium* (EfDapE) and *E. coli* (EfDapE). EfDapE is representative of Gram-positive bacteria while EcDapE is a homolog of the Gram-negative group. Although *E. coli* has not been labelled as an ESKAPE bacteria, it is a major cause of hard-to-treat urinary tract infections (UTI), while more recent evidences indicate the emergence in the last decades of gastrointestinal strains of this bacteria which are resistant to aminopenicillins and fluoroquinolones, commonly used to treat these infections; and thus, it should be argued that this species clearly belong to the multiresistant class of pathogens [33,34]. In the literature there are few studies regarding EcDapE [21,22,35] and none on EfDapE; moreover, the interaction of ORPH and DSF on DapE enzymes has also not been previously described or validated. Taken together, these results can help to understand the molecular mechanism of chemical-inhibition of DapE; and hence, consideration of critical interacting sites of the enzyme can assist in the design of selective and more effective of new anti-DapE compounds with conceivable antibacterial properties.

2. Materials and methods

2.1. Materials

Reagents, culture media, salts and buffers were purchased in Sigma-Aldrich. Restriction enzymes were from New England Biolabs. Gene synthesis and plasmid constructions were done by Genscript using the provided nucleotide sequences. Chromatographic columns were acquired from GE Healthcare. *E. coli* strain Bl21 pLys-DE3 for protein expression was from Promega.

2.2. Cloning, expression and purification of DapE recombinant enzyme

The entire gene sequences for DapE from *E. faecium* (UniProtKB: A0A133CNA8) and *E. coli were* cloned in-frame into the expression plasmid pET28b at the *Nde1* and *Xho1* restriction sites. Both recombinant enzymes were expressed and purified using the same protocol; which consists in overexpression in *E. coli* Bl21 pLys-DE3 strain transformed with the corresponding pET construct. Single colonies were inoculated into LB broth supplemented with appropriate antibiotic until the cell suspension reached stationary phase. For protein expression, saturated bacteria suspensions were diluted in fresh LB with kanamycin and cultured at 37 °C with aeration (vigorous shaking at 220 rpm) until the cell suspension reached an OD_{600nm} of 0.5. At this point, protein expression was induced with 0.2 mM of IPTG for 16 h at 20 °C under similar aeration conditions as before. Subsequently, cells were harvested by centrifugation at 6,000 rpm at 4 °C, and the pellet resuspended in lysis buffer (50 mM potassium phosphate buffer, 50 mM of KCl, 0.05 % v/v Triton X-100, 5 % v/v of glycerol, 1 mM of 2-mercaptoethanol, 30 mM of imidazole at pH= 8.0) and stored at −20 °C until further lysis and purification. Cell disruption was performed by sonication on ice of thawed suspensions at 10 μ, in 30 s pulses and 30 s of rest for 2 h period. Finally, the lysate was centrifuged at 12,000 rpm for 45 min at 4 °C and the supernatant containing the soluble fraction was filtered through a 0.45 μm syringe filter.

The cleared supernatant was loaded into a Ni^{2+} HiTrap HP column previously equilibrated with lysis buffer supplemented with 30 mM imidazole, and washed extensively with 10 volumes of 50

mM potassium phosphate buffer, 300 mM of KCl, 5 % v/v of glycerol, 1 mM of 2-mercaptoethanol and 30 mM of imidazole at pH 8.0. Proteins were eluted using an AKTA-Prime-Plus with the previous buffer supplemented with 300 mM of imidazole. Eluted protein fractions were analyzed by SDS-PAGE and those that contained pure DapE were pooled together and dialyzed using a 10 kDa Centricon® against 50 mM potassium phosphate buffer, 50 mM of KCl, 5 % v/v of glycerol, 1 mM of 2-mercaptoethanol pH 8.0, and stored at -80 °C.

2.3. Circular dichroism spectroscopy of enzyme preparations

The circular dichroism (CD) spectrum measurements for protein sample alone or in the presence of ligands were obtained using a Jasco J-810 spectropolarimeter (JASCO Corporation) equipped with a Peltier type cell holder and temperature control. The spectrum was obtained in the far UV region (200−250 nm). The concentration of the enzyme was 25 µg / mL in PBS at pH 8.0, deposited in a 0.5 cm optical cell at 22 °C, monitoring the changes in milligrades obtained at the different λ in nm.

2.4. Computational details

In order determine the type of compounds that can potentially interact with the DapE enzyme, an *in silic* ligand binding analysis was performed using the crystal structure of the HiDapE enzyme (PDB code: 3ic1) as a receptor, using the Dock Blaster tool [36], and the FDA-approved drugs of the ZINC database [37]. These tools have been used successfully in some similar studies for other targets [9,11,38]. The HiDapE active site cavity was automatically selected in the PDB calibration of the protein in the server and 500 different potentially-interacting drugs were inferred. From this list of potential DapE ligands, compounds with soft Lewis groups were identified and two drugs from this class, ORPH and DSF, were selected for further biochemical experiments given that they are both broadly used therapeutic FDA-approved drugs, with notable membrane permeability and multiple organs distribution as well as relatively low toxicity profiles in humans, and relevantly for metallohydrolases, they contain MBGś distributed in a co-planar configuration.

DSF is a drug originally used for the treatment of chronic alcoholism [39,40] with a long clinical history, which has allowed to document its side effects and its safety in its use [41–43]. Its molecular target that produces the adversity for alcohol is acetaldehyde dehydrogenase (ALDH-2) which DSF inactivates by blocking its catalytic cysteine [44]. It has been proposed as an antibacterial [45] and antiparasitic [46] agent and its ability to inhibit key enzymes essential for bacterial growth and viral replication has been demonstrated [45–51]. DSF has six soft heteroatoms which potentially interact with positively charged groups or weak Lewis acids, as is the case with DapE metal centers. ORPH is a drug in the antihistamine class, with anticholinergic effects. It was originally used to relieve muscle pain or wound pain, as well as to help regain motor control in Parkinson's patients [52]. It is considered a dirty drug, since it was identified that its action is through different molecular targets [53]. It is currently in five clinical trials, for purposes as a pain reliever in combination with other compounds. Drugs belonging to the group of antihistamines have been shown to be effective antibacterial agents, including for *E. faecium* and *E. coli* [54–57]. Anti-histamines could possess the ability to inhibit key enzymes for microbial growth [54–57]. ORPH possesses two heteroatoms that could interact with the DapE metal centers and present several π-bonds that could interact with the π-bonds containing groups located at enzyme active site. The rest of the potential inhibitors in the list do not meet all these characteristics, so it was decided to choose only these two drugs to test their interaction with DapE.

Binding sites for ligands in DapE enzyme were inferred by means of docking experiments in *H. influenzae* DapE (HiDapE), in the open (PDB code: 3ic1), partially closed (PDB code: 4pqa) and the closed (PDB code: 5vo3) conformations. Docking were performed using AutoDock Vina and by analyzing the nine best scored solutions [58] with the corresponding ligands. This tool has been used successfully to describe potential interactions *in silico* for other targets [11]. Ligand 3-D structures downloaded from Zinc Database as follows: orphenadrine citrate (code: ZINC565) and disulfiram (code: ZINC1529266). Three-dimensional structures were dock prepared using USCF-Chimera [59], followed by the function AutoDock Vina which was used to perform docking using a grid that corresponds to the whole dimeric structure. The most abundant auto-validated complex model was analyzed in USCF-Chimera and with LigPlot [60], and the best fitted model is presented.

2.5. Fluoresce binding experiments

Binding of polyphenols to DapE enzyme was monitored after apparent equilibrium by measuring changes in the intrinsic tryptophan fluorescence at 37 °C using a spectrometer (Fluostar Omega, BMG®). A sample of EfDapE at 0.05 mg/mL was excited at 290 nm, and fluorescence intensity was recorded at 340 nm after an hour of incubation at 37 °C in the absence or presence of different concentrations of ligands: ORPH and DSF. In order to discard solvent fluorescent changes, a control experiment was performed in which the different volumes of solvent (same as in the titration volumes used in ligand additions) were added to protein preparations. Fluorescence intensity changes were plotted against the ligand concentrations and fitted to Eq. (1).

Equation 1: Fluorescence binding saturation,

$$\Delta FI = (B_{max} * [ligand])/(K_d + [ligand]) \quad (1)$$

where ΔFI, is the change in fluorescence intensity at 340 nm; B_{max}, is the maximum ΔFI and corresponds to the maximum binding; [ligand], is the ligand concentration and K_d, is the dissociation constant. Additionally, fluorescence intensity data was analyzed using the modified Stern-Volmer equation (Eq. (2)), used to determine if the quenching is due to a single quenching mechanism [61,62].

Equation 2: Modified Stern-Volmer equation

$$\log(F_0 - F/F) = \log K_a + n \log[ligand] \quad (2)$$

where F_0, is the fluorescence intensity in the absence of ligand; F, is the fluorescence intensity in the presence of different concentrations of ligand; K_a, is the association constant of the ligand to the enzyme, and n is the number of ligand molecules that bind per protein molecule.

2.6. DapE thermostability in the absence and presence of ligands

In order to evaluate the thermostability of the DapE enzyme in the presence and absence of ligands, each recombinant protein was incubated in the native state with the SYPRO orange dye and the Solubility & Stability Screen 2^{TM} kit in a 96-well PCR microplate for 2 min at 25 °C, using a real-time-PCR instrument (StepOnePlus system from Applied Biosystems^{TM}). After that, a gradual increase (1 °C / min) in temperature (range from 25 to 98 °C) was applied, and the fluorescence emission of SYPRO Orange was monitored at a λ_{ex} of 470 nm while the thermal denaturation process of the protein occurred. This increase in temperature causes protein conformational changes that exposes hydrophobic, normally buried, residues resulting in increment of fluorescent signal; while this relationship of protein thermal-denaturation and fluorescence

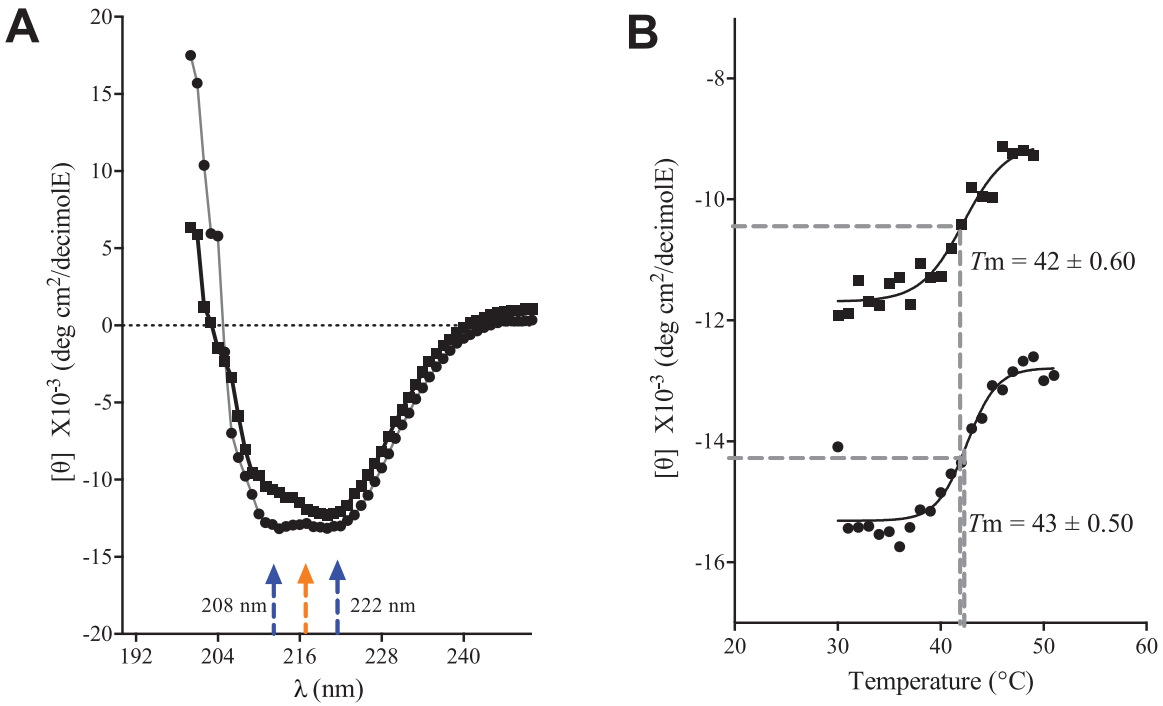

Fig. 1. EfDapE and EcDapE circular dichroism spectroscopic characterization. (A) circular dichroism spectra showing the consistency with an α/β protein, (B) Thermal stability followed by changes at molar ellipticity upon heating the protein sample. (●) corresponds to EfDapE and (■) to EcDapE.

emission can be used to estimate the apparent melting temperature in °C (apT_m) of DapE; conceivably, by compering this parameter of the enzyme in the absence and presence of the ligand we can infer a measurement of the thermal stability upon binding to the drug, as previously reported [63]. Complementary, thermal denaturation of DapE was additionally followed through changes in protein ellipticity at 222 nm. The temperature range used was and 25 to 90 °C controlled by the Peltier, which constantly increased the temperature at a speed of heating of 1 °C / min in a Jasco J-810 spectropolarimeter.

2.7. DapE inhibition by orphenadrine and disulfiram

A kinetic of inhibition of the DapE enzyme was performed following the hydrolysis rate of 0.5 mM of the esterase and peptidases analogous substrate, 4-nitrophenyl acetate, monitoring the absorbance at 405 nm in a FluoStar® Omega microplate spectrophotometer. The determination of the apparent constants of inhibition (IC_{50}) of DapE by the drugs were obtained from curve fit of the data to Eq. (3)

Equation 3: inhibition kinetics,

$$\text{Activity} = \text{Act0} * (IC_{50})/(IC_{50} + \text{I}) + \text{vr} \quad (3)$$

where IC_{50} is the apparent inhibition constant; [I], is the inhibitor concentration; Act0 is the activity in the absence of inhibitor and vr, is the activity observed at saturation of enzyme with inhibitor.

3. Results and discussion

3.1. Recombinant DapE preparation

EfDapE and EcDapE enzymes were purified to apparent homogeneity followed by structural verification of their native state by measuring their circular dichroism spectrum in the far UV region (200-250 nm) at 22 °C (Fig. 1A). The data obtained were analyzed on the commonly used (according to CrossRef has 393 citations for instance [64–66]) and validated public access web server K2D3 [67] yielded content ratios of α-helices and β-strands, consistent with those reported in the literature for known protein homologs (Table 1). To explore the thermal stability of the two enzymes, the molar ellipticity signal at 222 nm was followed upon gradual increments of sample temperature. We observed an apparent melting temperature (apT_m) of 43 ± 0.50 °C for EfDapE and 42 ± 0.60 °C for EcDapE (Fig. 1B), which are consistent with the optimum growth temperature of *E. faecium* and *E. coli*. Although in the current literature there are no data regarding the thermal stability of DapE enzymes for comparison, the apT_ms obtained are consistent with the temperatures normally used for the functional biochemical assays of DapE [13,15–24]. Values are also consistent with the calculated thermal stability of the proteins and the proteome of mesophilic organisms [68]. Given these observed structural features, we assume that the purified recombinant enzymes are in an adequate folding state, and relevantly, they provide useful preparations for the subsequent binding and inhibition experiments.

3.2. Binding experiments

The potential interaction of EfDapE and EcDapE with DSF and ORPH was assayed by measuring the quenching-effect of intrinsic tryptophan fluorescence upon the addition of the drugs, a spectrophotometrical technique that has previously been used with success and is useful to monitor and characterize the binding of ligand, including several enzyme-inhibitory drugs complex [48,61,62,69–72]. As expected, loss in intrinsic fluorescence intensity was observed following incubation of the enzymes with the both compounds, proportionally to the concentration of the drug being used, and following a hyperbolic trend. Changes in the fluorescence intensity ($\Delta FI = FI_{observed} - FI_{initial}$) were plotted versus ligand concentration; and the data obtained were fitted by nonlinear regression to Eq (1) (Fig. 2). The binding parameters obtained were dissociation constant (K_d) for the drug in question and the B_{max}, which is directly related to the conformational changes that occur in the enzyme after interacting with the drug. We observed K_d values in the range of μM for both drugs. This obser-

Table 1
DapE secondary structure content of some DapE enzymes, as well as for EfDapE and EcDapE.

PDB code	α-helices %	β- strands %	Reference	PDB code	α-helices %	β- strands %	Reference
1VGY	30	26	[87]	4O23	30	27	[26]
3IC1	31	25	[23]	4ONW	36	21	[16]
3ISZ	32	25	[23]	4OP4	36	21	[16]
3KHX	28	21	[88]	4PPZ	30	27	[26]
3KHZ	28	23	[88]	4PQA	30	27	[26]
3KI9	30	25	[88]	5UEJ	30	27	[89]
3PFE	39	22	[90]	5VO3	32	26	[16]
3TX8	29	27	[91]	EcDapE[a]	22	27	This study
4H2K	34	19	[16]	EfDapE[a]	28	25	This study

[a] Data obtained experimentally by CD analysis compared with the structures contained in the PDB with known secondary structure content.

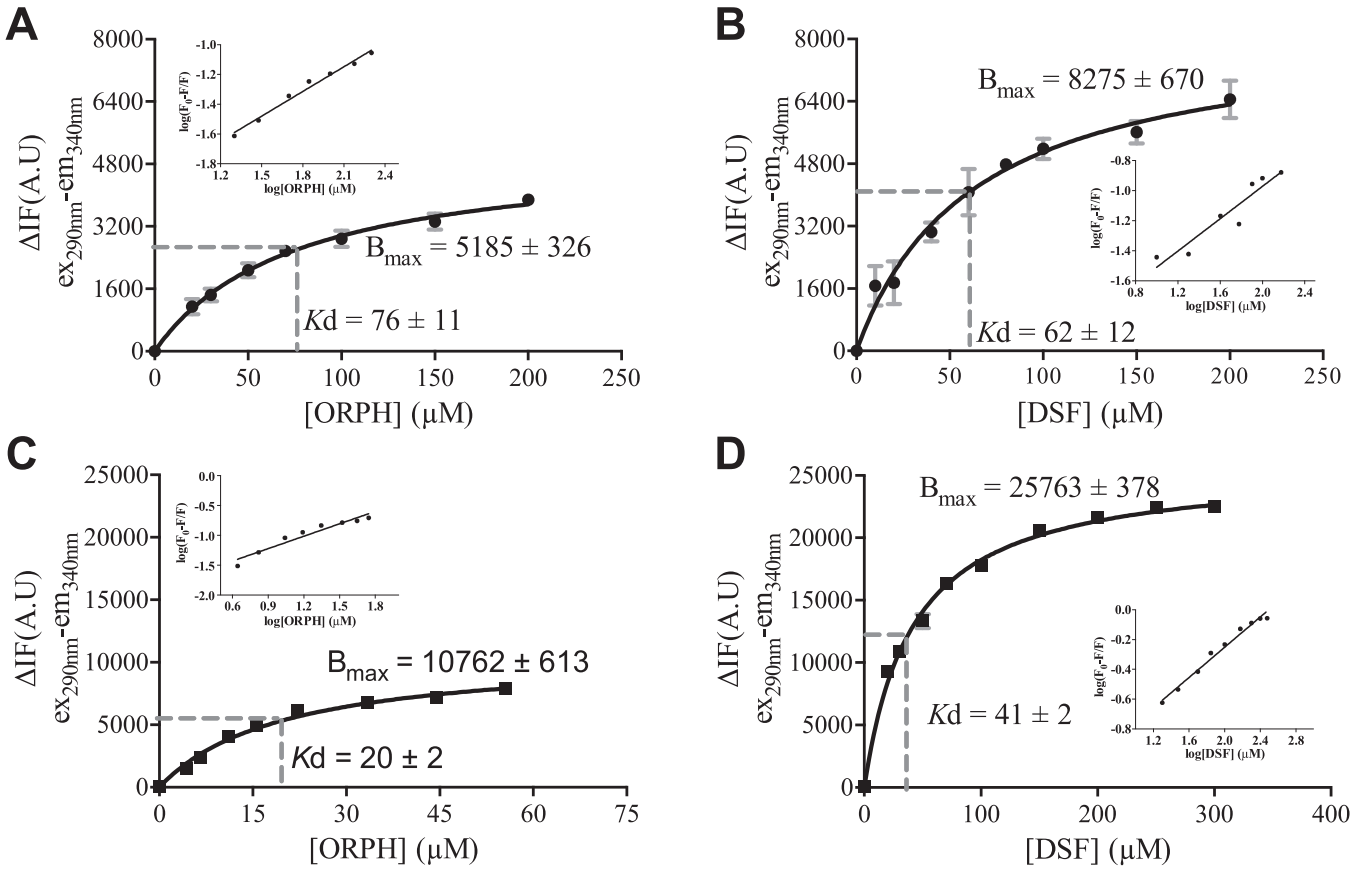

Fig. 2. Drug binding into DapE enzymes. (A) EfDapE saturation by ORPH, and (B) by and DSF, (C) EcDapE saturation by ORPH, and (D) by DSF. Fluorescence changes are plotted against the drug concentration used. Three independent experiments were performed and mean, and error bars are depicted. Symbols are de experimental data and continuous line is the best curve fit to Eq. (2). Binding parameters are shown in graphs, dashed lines indicate the inflection points. Excitation (ex) and emission (em) wavelengths are indicated. Inserts corresponds to Stern-Volmer plots using fluorescence intensity of enzymes in the absence (F_0) and fluorescence intensities in the presence of drugs.

vation is to some extent comparable with some values reported in binding studies of DapE with other ligands [20,27]. A modified Stern-Volmer analysis was performed with the ligand binding data measured by fluorescence intensities (Fig. 2-inserts). The linear trend of the curves suggests that a single quenching event is occurring during the drug binding process in DapE enzymes. The change in fluorescence caused by DSF binding is greater than that caused by ORPH (inferred as a greater conformational change), which results into a higher B_{max}/ K_d ratio for DSF, indicating a potential greater specificity for DSF. This apparent distinct specificity may be due to differences in volume/steric hindrance of drugs or the presence and number of groups/heteroatoms capable of interacting with the metal centers, since ORPH has only two, whereas the DSF has six. These findings give us a clue to the potential of the sulfur atom, which are consistent with observations reported on other studies [20,26]. Given this chemical property, in future studies it would be of great interest to carry out a more exhaustive search for additional compounds that possess sulfur-based functional groups that could interact with Zn-centers. In addition, those interacting atoms in DSF are notably accommodated in a similar pattern, as the MBG present in the substrate NSDAP (Fig. 3).

Relevantly, during the performance of the binding experiments, we observed the formation of aggregates following incubation for long periods at room temperature with both drugs, the addition of which presumably resulted in protein precipitation. To further investigate if the precipitation, presumably of the enzyme-ligand complex, is related to changes in the stability of the enzyme in the complex, we determined the thermal stability through thermo-

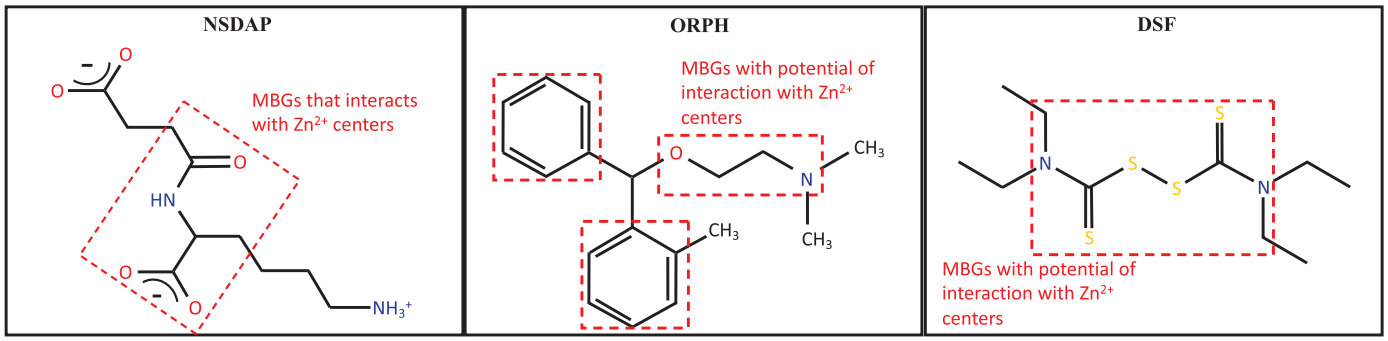

Fig. 3. Substrate, ORPH and DSF structures. Physiological substrate N-succinyl-L,L-diaminopimelate (NSDAP) is shown for reference in order to compare for structural similarities with drugs.

fluorescence assay and recorded the changes in the apT_m of the complexes with respect to that of the enzyme alone. Thermo fluorescence assays (TF) or also called thermal shift assays have been widely used to identify and characterize interactions between proteins and ligands, including molecular targets and drugs [63,73]. In most cases, it has been documented that the binding of a ligand or a drug to a protein produces an increase in receptor stability, which can be observed by an increase in its thermal stability deduced from the increment in the protein denaturation T_m parameter [73]. Nonetheless, it has been occasionally observed that the binding of a ligand/drug results in a decrease in the stability of the macromolecular receptor and a corresponding reduction in its T_m [74–76]. Consequently, the effect of drug binding to a particular protein can either further stabilize or destabilize the native structure of the receptor. Given that the binding of ORPH and DSF in the model DapE enzymes produced an aggregation phenomenon after long incubation periods, we hypothesized that these drugs induce an enzyme destabilization.

The observed apT_m value of the enzymes alone in the thermal shift assay was approximately 40 °C, values consistent with those found by circular dichroism measured at the 222 nm wavelength peak (corresponding to a loss of alpha-helical secondary structure). Upon binding of either DSF or ORPH, a drop in in thermal stability was observed. The loss of protein stability produced by ORPH was higher, given that the enzyme showed a high fluorescence with the SYPRO-Orange even at the lowest temperatures assessed. This characteristic is reportedly found in partially denatured proteins, in which buried hydrophobic residues that interact with the fluorescence dye are readily exposed at low temperatures [77]. Considering that it was difficult to quantify protein destabilization in the standard buffer condition, due to high fluorescence intensity we repeated this assay using citrate buffer (1M tribasic sodium citrate dihydrate at pH 5.0). This buffer was selected based on the higher observable stability of the enzyme in the absence of ligands, following screening of several conditions of the Solubility & Stability Screen 2^{TM}. Under these more optimal conditions, addition of DSF to both DapE enzyme resulted in a change of the estimated apT_m (ΔT_m) of −11.90 °C for EfDapE and −15.60 °C for EcDapE, when compared to that of the enzyme alone (Table 2). The protein destabilization effect by ORPH was −18.00 °C for EcDapE, while for EfDapE was not possible to estimate the change, given the high-level of fluorescence shown at room temperature, hence, although both drugs promote protein destabilization, we assume a larger effect by ORPH. Overall, these estimated destabilization effects are consistent with the visible rapid formation of purified protein precipitates upon incubation with the two tested compounds. These observations may be relevant for their potential use as antimicrobial agents, since the generation of protein aggregation phenomena can generate additional stressful and harmful conditions in target cells; hence, these protein destabilizing drugs present an advantage over another compound that only inhibit the target enzyme.

Table 2
Thermal stability for EfDapE and EcDapE.

	Standard buffer			Citrate buffer
Enzyme	CD-apT_m (°C)	TF-apT_m (°C)	ΔT_m (°C)	ΔT_m (°C)
EfDapE	43.00	40.10	–[b]	–
EcDapE	42.00	41.00	–	–
EfDapE-ORPH	npd[a]	36.39	-3.71	npd
EfDapE-DSF	npd	39.77	-0.33	11.90
EcDapE-ORPH	npd	36.71	-4.29	17.97
EcDapE-DSF	npd	40.05	-0.95	15.60

[a] Not possible to determinate.
[b] does not apply.

Once we determined the interaction capacity of ORPH and DSF into EfDapE and EcDapE, we investigated whether binding to these compounds were sufficient to inhibit the activity of the enzymes. The effect on enzyme activity upon incubation against increasing concentrations of both drugs was followed over the rate of hydrolysis of 4-nitrophenyl acetate (fixed concentration of 500 μM). We observed that both compounds caused the gradual loss of activity in accordance to their concentration used (Fig. 4). The data obtained were plotted and non-linear fitted to Eq. (3). IC_{50} values obtained in these experiments are consistent with those observed in dissociation constants determined from the fluorescence-binding experiments. The IC_{50} values of other DapE inhibitors are in the range of 3 to 1000 μM. The inhibition values on DapE function that we found for these two drugs are close to those previously reported [20] for 4-mercaptobutyric acid (43 μM), 3-mercaptobenzoic acid (21.8 μM), thiopheneboronic acid (34 μM) and penicillamine (13.7 μM). Although the obtained IC_{50} values are not those expected for a potential antibiotic, it can be highlighted that the characterization we present provides us with clues for the search and discovery of a new type of inhibitors. An additional desired chemical property for these two compounds is that they are relatively hydrophobic, with a high potential to cross the plasma membranes of bacteria, both Gram-positively and more relevant, Gram-negative organisms, to access to the cytoplasmatic target enzyme, DapE.

As far as is known, from the known DapE inhibitors only captopril, enapril and penicillamine are drugs approved for use in humans according to DrugBank [30]. Although DSF, like many drugs, has side effects and contraindications, it can be administered in doses of up to 0.8 g per day [42], which in some way guarantees that it reaches effective concentrations in the serum, however, its use as an antibiotic still requires numerous *in vitro* tests and clinical trials to further address its effectiveness and safety.

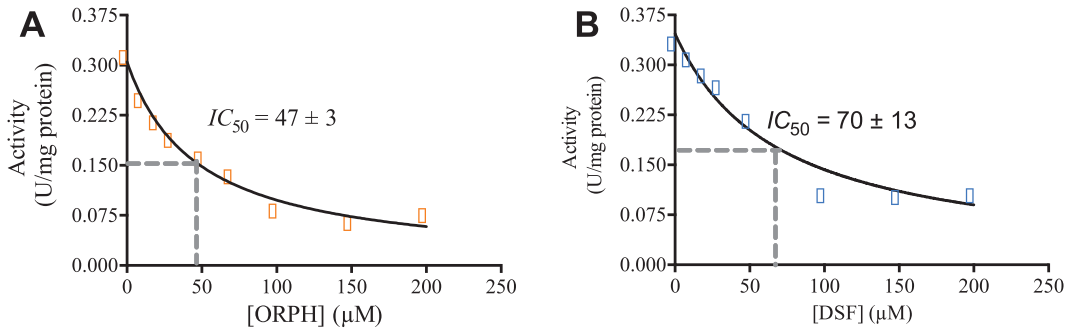

Fig. 4. Inhibition kinetics of EfDapE by (A) ORPH and (B) DSF. Activity changes are plotted against the drug concentration used. Three independent experiments were performed, and mean is depicted. Symbols are de experimental data and continuous line is the best curve fit to Eq. (3).

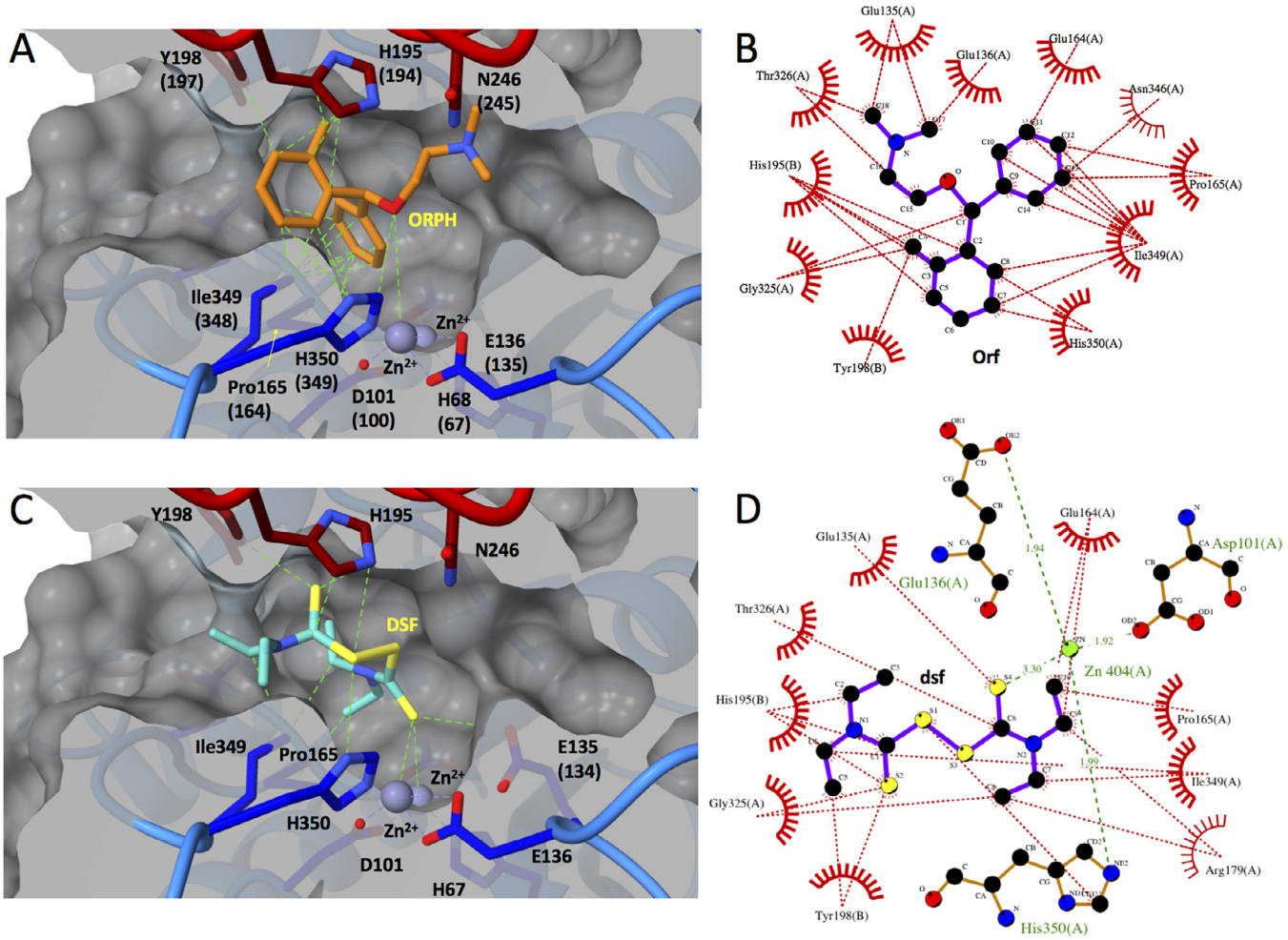

Fig. 5. DapE-drug complex model analysis. (A) Depiction of interactions between ORPH and DapE active site, showing relevant aminoacid residues, (B) LigPlot analysis of DapE-ORPH binding complex, (C) Depiction of interactions between DSF and DapE active site, showing relevant aminoacid residues (PDB code: 4pqa), (D) LigPlot analysis of DapE-ORPH binding complex. For A and C, chartreuse dashed lines indicate interaction describes in Section 3.3; for (B) and (D), red dashed lines represent hydrophobic interaction between connected atoms and green dashed lines represent polar interactions. Corresponding subunits of protein dimer are indicated by letters in parenthesis. Three code letter nomenclature for aminoacids and position in DapE from *Neisseria meningitidis and in parentheses for* and aHiDapE are shown, drugs are depicted in sticks representation and HiDapE is shown as surface representation to identify cavity and in ribbons to map residues positions and chains. Images for A and C were obtained using USCF-Chimera and for B and D using LigPlot.

3.3. Potential sites of interactions of the enzyme with the drugs

Molecular docking experiments were performed and inferred that both compounds had a high potential interaction with the active site of DapE (Fig. 5). Both, ORPH (Fig. 5A and B) and DSF (Fig. 5C and D), interact with residues located in the active site through the following non-polar interactions: In the DapE-ORPH complex model, these can be classified into two types (Fig. 5A and B): (1) hydrophobic interactions, which are observed between the methyl δ of Ile349 and both phenyl rings of ORPH, and between the γ and δ carbons of Pro165 with ring A; (2) dispersion forces or π-stacking, observed between the imidazole ring of His195 and

various carbons of the B ring of ORPH, between the phenolic ring of Y198 and B ring of the ligand, and between the amidic nitrogen δ of Asn346 and ring A of ORPH. The second type of interaction are recognized as important in the molecular recognition between proteins and ligands in other systems [78–82]. Additionally, an interaction is observed between the oxygen of the ligand and the carbon ε of the imidazole of His350, an atom that has part of the delocalized charge of histidine, and a potential interaction between this same oxygen and the metal center-2, but the distance between these two atoms is 4.7 Å and could only occur if the oxygen atom is accommodated deeper inside.

The following non-covalent interactions are observed in the DapE-DSF complex: one between a thionyl group and metal center 2 (at 3.3 Å, which is in the range of a polar interaction), this thionyl is at a distance of 3.7 Å from both the center 1 and the Glu135 carboxyl group (could be dispersion forces); one of the disulfide bonds of the DSF, interacts with the imidazole group of His197 and at the same time with His350, both at a distance of 4.0 Å; the other thionyl group potentially it is bound by π-stacking with His195 and Tyr198 rings; two of the methylene groups in the lateral parts of DSF, interact hydrophobically with the methyl δ of Ile349 and finally one of the methyl of the ligand is stabilized by the CH δ of the Pro165. (Fig. 5C and D). Remarkably, the binding of these drugs is observed in both, the open and the partially closed forms of the DapE enzyme, but not into the full-closed form. Three-dimensional structures of DapE enzymes has been observed between two states, called the open and closed conformations [16]. Open conformations were described extensively in the literature and the fully closed form was observed recently in DapE–N-diaminopimelate–succinate complex [16]. It was hypothesized that substrate binding into the open state, induces a conformational transition that leads to closed-form [16,83]. Two aspects are functionally relevant concerning for this transition. Firstly, the catalytic His195, located in the oligomerization domain of the opposite chain to one of the active sites, enters and allows the assembly of the oxyanion hole, which is necessary for the stabilization of the transient-negative-charge of product intermediate [16]; secondly, other residues from the opposite chain also enters into the active site and interact with other functional groups of the substrate, allowing its stabilization [16]. These findings highlighted important features in the selection or design of new anti-DapE compounds [16]. Consequently, there could be at least two types of optimal inhibitors: those that after binding to any of the open forms of DapE, interfere with enzyme induced fit, hence blocking the entry of relevant residues for recognition and catalysis; another type of ligand are those that eliminate the functional properties of critical active site determinants by interacting with them. A possible guide for selecting both types of compounds could be inferred from binding compatibilities in different enzyme states, deduced from docking or crystallographic experiments. Inhibitors that can only bind into active sites of the DapE open form in molecular docking or if in co-crystallization is only observed in the open or partially open conformations, is indicative of a ligand that interfere with the induced fit. Contrary, if it is compatible with both, the open and closed conformations, is indicative of an inhibitor that eliminates the functional properties of the enzyme but does not bocks the closure transition. Concerning ORPH and DSF binding, we found that interaction it is only compatible with DapE active site in the fully open (PDB code: 3ic1) and to the partially closed (PDB code: 4pqa) forms but not in the fully closed state (PDB code: 5vo3), suggesting that the binding of both drugs prevents the optimal and productive closure of the enzyme. Furthermore, these drugs interact with critical residues located in the catalytic domain, and consequently also interfere with the optimal functioning of these critical groups by blocking the active site, and thus, preventing the accommodation of the substrate into the productive position. There are some reports of ligands that act both with open and closed forms of other enzymes, for instance [84–86].

Both drugs are positioned in the cleft of the active site between the residues of the two subunits that structure the productive form of the active site, blocking the functioning of the catalytic residues: His195, Glu135, as well as residues that participate in the stabilization of the metal centers: Glu136, Glu164 and His350. It had been previously stipulated that anti-DapE agents must present groups capable of binding to metals of the enzyme but also polar and ionic residues at the active site through extensive polar non-covalent interactions; however, in this study we show the inhibitory potential of groups with relative hydrophobicity and that lack those model features. However, one sulfur atom present in the thionyl group of the DSF is a weak Lewis base that can interact with the metal center, preventing its role in catalysis, and more specifically in its function as part of the oxyanion hole of the enzyme. We also found that Ile349, Pro165, Tyr197, and His195 could be key structural determinants in the recognition of ligands, including inhibitors, therefore in future studies, it is important also to pay attention to these amino acid residue positions for selection and identification of new DapE inhibitors.

4. Conclusion

DSF and ORPH are DapE ligands and inhibitors. The binding of these drugs into EfDapE and EcDapE resulted also in a decrease in protein stability that leads to protein aggregation after a period of incubation. This effect may present an advantage for the application of these drugs into pathogen bacteria since protein aggregation can result in harmful irreversible stress, besides the activity inhibitory capacity of drugs. These FDA-approved drugs appear to bind into enzyme mainly due to hydrophobic interactions. The information presented in this study provides structural features with respect to the functional groups, of both enzyme and inhibitors, potentially critical for inhibition and can be used for further design and develop of new class of antimicrobial agents.

Declaration of Competing Interest

Authors declare no conflict of interest.

CRediT authorship contribution statement

Manuel Terrazas-López: Investigation, Conceptualization, Validation, Formal analysis. **Naún Lobo-Galo:** Conceptualization, Writing - original draft, Writing - review & editing. **Luis Guadalupe Aguirre-Reyes:** Investigation, Validation. **Ismael Bustos-Jaimes:** Methodology, Conceptualization, Formal analysis, Resources. **Jorge Ángel Marcos-Víquez:** Investigation, Formal analysis. **Lilian González-Segura:** Methodology, Conceptualization, Formal analysis, Resources. **Ángel Gabriel Díaz-Sánchez:** Conceptualization, Formal analysis, Writing - original draft, Writing - review & editing, Funding acquisition.

Acknowledgments

This work was supported by the Nacional Council of Science and technology: "Consejo Nacional de Ciencia y Tecnología" (CONACYT) from Mexican Government, through the program "*Proyecto de Desarrollo Científico para Atender Problemas Nacionales*": [grant number CONACYT-PN-2015-587]. Manuel Terrazas-Lopez received a fellowship for a master's and another for a PhD degree by CONACYT-National Fellowship Program.

References

[1] N.I. Paphitou, Antimicrobial resistance: action to combat the rising microbial challenges, Int. J. Antimicrob. Agents 42 (2013) S25–S28, doi:10.1016/j.ijantimicag.2013.04.007.

[2] M.E.A. de Kraker, A.J. Stewardson, S. Harbarth, Will 10 million people die a year due to antimicrobial resistance by 2050? PLOS Med. 13 (2016) e1002184, doi:10.1371/journal.pmed.1002184.

[3] L.B. Rice, Federal funding for the study of antimicrobial resistance in nosocomial pathogens: no ESKAPE, J. Infect. Dis. 197 (2008) 1079–1081, doi:10.1086/533452.

[4] L.M. Weiner, A.K. Webb, B. Limbago, M.A. Dudeck, J. Patel, A.J. Kallen, J.R. Edwards, D.M. Sievert, Antimicrobial-resistant pathogens associated with healthcare-associated infections: summary of data reported to the National Healthcare Safety Network at the centers for disease control and prevention, 2011-2014, Infect. Control Hosp. Epidemiol. 37 (2016) 1288–1301, doi:10.1017/ice.2016.174.

[5] C. Suetens, K. Latour, T. Kärki, E. Ricchizzi, P. Kinross, M.L. Moro, B. Jans, S. Hopkins, S. Hansen, O. Lyytikäinen, J. Reilly, A. Deptula, W. Zingg, D. Plachouras, D.L. Monnet, Prevalence of healthcare-associated infections, estimated incidence and composite antimicrobial resistance index in acute care hospitals and long-term care facilities: results from two European point prevalence surveys, 2016 to 2017, Eurosurveillance 23 (2018) 1800516, doi:10.2807/1560-7917.ES.2018.23.46.1800516.

[6] F.M. Mobegi, S.A.F.T. van Hijum, P. Burghout, H.J. Bootsma, S.P.W. de Vries, C.E. van der Gaast-de Jongh, E. Simonetti, J.D. Langereis, P.W.M. Hermans, M.I. de Jonge, A Zomer, From microbial gene essentiality to novel antimicrobial drug targets, BMC Genom. 15 (2014) 958, doi:10.1186/1471-2164-15-958.

[7] S.E. Maddocks, Novel targets of antimicrobial therapies, Microbiol. Spectr. 4 (2016), doi:10.1128/microbiolspec.vmbf-0018-2015.

[8] V.M. Chernov, O.A. Chernova, A.A. Mouzykantov, L.L. Lopukhov, R.I. Aminov, Omics of antimicrobials and antimicrobial resistance, Expert Opin. Drug Discov. 14 (2019) 455–468, doi:10.1080/17460441.2019.1588880.

[9] H.B. Samal, J.K. Das, R.K. Mahapatra, M. Suar, Molecular modeling, simulation and virtual screening of MurD ligase protein from Salmonella typhimurium LT2, J. Pharmacol. Toxicol. Methods. 73 (2015) 34–41, doi:10.1016/j.vascn.2015.03.005.

[10] J.J. Irwin, B.K. Shoichet, M.M. Mysinger, N. Huang, F. Colizzi, P. Wassam, Y. Cao, Automated docking screens: a feasibility study, J. Med. Chem. (2009), doi:10.1021/jm9006966.

[11] K. Anbarasu, S. Jayanthi, Designing and optimization of novel human LMTK3 inhibitors against breast cancer–a computational approach, J. Recept. Signal Transduct. 37 (2017) 51–59, doi:10.3109/10799893.2016.1155069.

[12] D.M. Gillner, D.P. Becker, R.C. Holz, Lysine biosynthesis in bacteria: a metallodesuccinylase as a potential antimicrobial target, JBIC J. Biol. Inorg. Chem. 18 (2013) 155–163, doi:10.1007/s00775-012-0965-1.

[13] M. Karita, M.L. Etterbeek, M.H. Forsyth, M.K.R. Tummuru, M.J. Blaser, Characterization of Helicobacter pylori dapE and construction of a conditionally lethal dapE mutant, Infect. Immun. (1997) https://iai.asm.org/content/65/10/4158.long.

[14] M.S. Pavelka, W.R. Jacobs, Comparison of the construction of unmarked deletion mutations in Mycobacterium smegmatis, Mycobacterium bovis bacillus Calmette-Guerin, and Mycobacterium tuberculosis H37RV by allelic exchange, J. Bacteriol. (1999), doi:10.1128/jb.181.16.4780-4789.1999.

[15] T.L. Born, R. Zheng, J.S. Blanchard, Hydrolysis of N -Succinyl- L, L -diaminopimelic Acid by the Haemophilus influenzae dapE -Encoded Desuccinylase: Metal Activation, Solvent Isotope Effects, and Kinetic Mechanism †, Biochemistry 2960 (1998) 10478–10487.

[16] B. Nocek, C. Reidl, A. Starus, T. Heath, D. Bienvenue, J. Osipiuk, R. Jedrzejczak, A. Joachimiak, D.P. Becker, R.C. Holz, Structural evidence of a major conformational change triggered by substrate binding in DapE enzymes: impact on the catalytic mechanism, Biochemistry 57 (2018) 574–584, doi:10.1021/acs.biochem.7b01151.

[17] N.J. Cosper, D.L. Bienvenue, J.E. Shokes, D.M. Gilner, T. Tsukamoto, R.A. Scott, R.C. Holz, The dapE-encoded N-Succinyl-L,L-Diaminopimelic Acid Desuccinylase from Haemophilus influenzae Is a Dinuclear Metallohydrolase, J. Am. Chem. Soc. 125 (2003) 14654–14655, doi:10.1021/ja036650v.

[18] R. Davis, D. Bienvenue, S.I. Swierczek, D.M. Gilner, L. Rajagopal, B. Bennett, R.C. Holz, Kinetic and spectroscopic characterization of the E134A- and E134D-altered dapE-encoded N-succinyl-l,l-diaminopimelic acid desuccinylase from Haemophilus influenzae, JBIC J. Biol. Inorg. Chem. 11 (2006) 206–216, doi:10.1007/s00775-005-0071-8.

[19] D. Dutta, S. Mishra, Active site dynamics in substrate hydrolysis catalyzed by DapE enzyme and its mutants from hybrid QM/MM-molecular dynamics simulation, J. Phys. Chem. B. 121 (2017) 7075–7085, doi:10.1021/acs.jpcb.7b04431.

[20] D. Gillner, N. Armoush, R.C. Holz, D.P. Becker, Inhibitors of bacterial N-succinyl-l,l-diaminopimelic acid desuccinylase (DapE) and demonstration of in vitro antimicrobial activity, Bioorg. Med. Chem. Lett. 19 (2009) 6350–6352, doi:10.1016/j.bmcl.2009.09.077.

[21] F. Javid-Majd, J.S. Blanchard, Mechanistic analysis of the argE-Encoded N-Acetylornithine Deacetylase †, Biochemistry 39 (2000) 1285–1293, doi:10.1021/bi992177f.

[22] W.C. McGregor, D.M. Gillner, S.I. Swierczek, D. Liu, R.C. Holz, Identification of a Histidine Metal Ligand in the argE-Encoded N-Acetyl-L-Ornithine Deacetylase from Escherichia coli, Springerplus 2 (2013) 482, doi:10.1186/2193-1801-2-482.

[23] B.P. Nocek, D.M. Gillner, Y. Fan, R.C. Holz, A. Joachimiak, Structural basis for catalysis by the mono- and dimetalated forms of the dapE-Encoded N-succinyl-l,l-Diaminopimelic Acid Desuccinylase, J. Mol. Biol. 397 (2010) 617–626, doi:10.1016/j.jmb.2010.01.062.

[24] B. Nocek, A. Starus, M. Makowska-Grzyska, B. Gutierrez, S. Sanchez, R. Jedrzejczak, J.C. Mack, K.W. Olsen, A. Joachimiak, R.C. Holz, The dimerization domain in dape enzymes is required for catalysis, PLoS One (2014) 9, doi:10.1371/journal.pone.0093593.

[25] N.R. Uda, G. Upert, G. Angelici, S. Nicolet, T. Schmidt, T. Schwede, M. Creus, Zinc-selective inhibition of the promiscuous bacterial amide-hydrolase DapE: implications of metal heterogeneity for evolution and antibioticdrug design, Metallomics 6 (2014) 88–95, doi:10.1039/C3MT00125C.

[26] A. Starus, B. Nocek, B. Bennett, J.A. Larrabee, D.L. Shaw, W. Sae-Lee, M.T. Russo, D.M. Gillner, M. Makowska-Grzyska, A. Joachimiak, R.C. Holz, Inhibition of the dapE-Encoded N-Succinyl-L,L-diaminopimelic Acid Desuccinylase from Neisseria meningitidis by L-Captopril, Biochemistry 54 (2015) 4834–4844, doi:10.1021/acs.biochem.5b00475.

[27] T.K. Heath, M.R. Lutz, C.T. Reidl, E.R. Guzman, C.A. Herbert, B.P. Nocek, R.C. Holz, K.W. Olsen, M.A. Ballicora, D.P. Becker, Practical spectrophotometric assay for the dapE-encoded N-succinyl-L,L-diaminopimelic acid desuccinylase, a potential antibiotic target, PLoS One 13 (2018) e0196010, doi:10.1371/journal.pone.0196010.

[28] B. Nocek, A. Starus, M. Makowska-Grzyska, B. Gutierrez, S. Sanchez, R. Jedrzejczak, J.C. Mack, K.W. Olsen, A. Joachimiak, R.C. Holz, The dimerization domain in DapE enzymes is required for catalysis, PLoS One 9 (2014) e93593, doi:10.1371/journal.pone.0093593.

[29] T.K. Heath, The Enzymatic Activity and Inhibition of DapE Encoded N-Succinyl-L,l-Diaminopimelic Acid Dessucinylase, Loyola University Chicago, 2018 https://ecommons.luc.edu/luc_diss/2811/.

[30] D.S. Wishart, C. Knox, A.C. Guo, D. Cheng, S. Shrivastava, D. Tzur, B. Gautam, M. Hassanali, DrugBank: a knowledgebase for drugs, drug actions and drug targets, Nucleic Acids Res 36 (2008) D901–D906, doi:10.1093/nar/gkm958.

[31] M. Akif, D. Georgiadis, A. Mahajan, V. Dive, E.D. Sturrock, R.E. Isaac, K.R. Acharya, High-resolution crystal structures of drosophila melanogaster angiotensin-converting enzyme in complex with novel inhibitors and antihypertensive drugs, J. Mol. Biol. 400 (2010) 502–517, doi:10.1016/j.jmb.2010.05.024.

[32] R.S. Mandal, S. Das, In silico approach towards identification of potential inhibitors of Helicobacter pylori DapE, J. Biomol. Struct. Dyn. (2015), doi:10.1080/07391102.2014.954272.

[33] V.P. O'Brien, T.J. Hannan, H.V. Nielsen, S.J. Hultgren, Drug and vaccine development for the treatment and prevention of urinary tract infections, Microbiol. Spectr. 4 (2016), doi:10.1128/microbiolspec.UTI-0013-2012.

[34] W.E. van der Starre, C. van Nieuwkoop, S. Paltansing, J.W. van't Wout, G.H. Groeneveld, M.J. Becker, T. Koster, G.H. Wattel-Louis, N.M. Delfos, H.C. Ablij, E.M.S. Leyten, J.W. Blom, J.T. van Dissel, Risk factors for fluoroquinolone-resistant Escherichia coli in adults with community-onset febrile urinary tract infection, J. Antimicrob. Chemother. 66 (2011) 650–656, doi:10.1093/jac/dkq465.

[35] J. Bouvier, C. Richaud, W. Higgins, O. Bögler, P. Stragier, Cloning, characterization, and expression of the dapE gene of Escherichia coli, J. Bacteriol. 174 (1992) 5265–5271, doi:10.1128/JB.174.16.5265-5271.1992.

[36] J.J. Irwin, B.K. Shoichet, M.M. Mysinger, N. Huang, F. Colizzi, P. Wassam, Y. Cao, Automated docking screens: a feasibility study, J. Med. Chem. 52 (2009) 5712–5720, doi:10.1021/jm9006966.

[37] J.J. Irwin, T. Sterling, M.M. Mysinger, E.S. Bolstad, R.G. Coleman, ZINC: a free tool to discover chemistry for biology, J. Chem. Inf. Model. (2012), doi:10.1021/ci3001277.

[38] L. Allam, G. Fatima, L. Wiame, H. El Amri, A. Ibrahimi, Molecular screening and docking analysis of LMTK3 and AKT1 combined inhibitors, Bioinformation 14 (2018) 499–503, doi:10.6026/97320630014499.

[39] R.K. Fuller, H.P. Roth, Disulfiram for the treatment of alcoholism. An evaluation in 128 men, Ann. Intern. Med. 90 (1979) 901–904, doi:10.7326/0003-4819-90-6-901.

[40] R.K. Fuller, W.O. Williford, K.K. Lee, R. Derman, Veterans administration cooperative study of disulfiram in the treatment of alcoholism: study design and methodological considerations, Control. Clin. Trials 5 (1984) 263–273, doi:10.1016/0197-2456(84)90030-8.

[41] J.J. Suh, H.M. Pettinati, K.M. Kampman, C.P. O'Brien, The status of disulfiram: a half of a century later, J. Clin. Psychopharmacol. (2006), doi:10.1097/01.jcp.0000222512.25649.08.

[42] A. Yoshimura, M. Kimura, H. Nakayama, T. Matsui, F. Okudaira, S. Akazawa, M. Ohkawara, T. Cho, Y. Kono, K. Hashimoto, M. Kumagai, Y. Sahashi, S. Roh, S. Higuchi, Efficacy of disulfiram for the treatment of alcohol dependence assessed with a multicenter randomized controlled trial, Alcohol. Clin. Exp. Res. (2014), doi:10.1111/acer.12278.

[43] M.D. Skinner, P. Lahmek, H. Pham, H.J. Aubin, Disulfiram efficacy in the treatment of alcohol dependence: a meta-analysis, PLoS One (2014), doi:10.1371/journal.pone.0087366.

[44] J.J. Lipsky, M.L. Shen, S. Naylor, In vivo inhibition of aldehyde dehydrogenase by disulfiram, Chem. Biol. Interact. (2001), doi:10.1016/S0009-2797(00)00225-8.
[45] V.J. Zaldívar-Machorro, M. López-Ortiz, P. Demare, I. Regla, R.A. Muñoz-Clares, The disulfiram metabolites S-methyl-N,N-diethyldithiocarbamoyl sulfoxide and S-methyl-N,N-diethylthiocarbamoyl sulfone irreversibly inactivate betaine aldehyde dehydrogenase from Pseudomonas aeruginosa, both in vitro and in situ, and arrest bacterial grow, Biochimie 93 (2011) 286–295, doi:10.1016/j.biochi.2010.09.022.
[46] A. Galkin, L. Kulakova, K. Lim, C.Z. Chen, W. Zheng, I.V Turko, O. Herzberg, Structural basis for inactivation of Giardia lamblia carbamate kinase by disulfiram, J. Biol. Chem. 289 (2014) 10502–10509, doi:10.1074/jbc.M114.553123.
[47] A.G. Dalecki, M. Haeili, S. Shah, A. Speer, M. Niederweis, O. Kutsch, F. Wolschendorf, Disulfiram and copper ions kill mycobacterium tuberculosis in a synergistic manner, Antimicrob. Agents Chemother. 59 (2015) 4835–4844, doi:10.1128/AAC.00692-15.
[48] Á. Díaz-Sánchez, E. Alvarez-Parrilla, A. Martínez-Martínez, L. Aguirre-Reyes, J. Orozpe-Olvera, M. Ramos-Soto, J. Núñez-Gastélum, B. Alvarado-Tenorio, L. de la Rosa, Inhibition of urease by disulfiram, an FDA-approved thiol reagent used in humans, Molecules 21 (2016) 1628, doi:10.3390/molecules21121628.
[49] M.H. Lin, D.C. Moses, C.H. Hsieh, S.C. Cheng, Y.H. Chen, C.Y. Sun, C.Y. Chou, Disulfiram can inhibit MERS and SARS coronavirus papain-like proteases via different modes, Antiviral Res. (2018), doi:10.1016/j.antiviral.2017.12.015.
[50] Z. Jin, X. Du, Y. Xu, Y. Deng, M. Liu, Y. Zhao, B. Zhang, X. Li, L. Zhang, C. Peng, Y. Duan, J. Yu, L. Wang, K. Yang, F. Liu, R. Jiang, X. Yang, T. You, X. Liu, X. Yang, F. Bai, H. Liu, X. Liu, L.W. Guddat, W. Xu, G. Xiao, C. Qin, Z. Shi, H. Jiang, Z. Rao, H. Yang, Structure of Mpro from SARS-CoV-2 and discovery of its inhibitors, Nature 582 (2020) 289–293, doi:10.1038/s41586-020-2223-y.
[51] N. Lobo-Galo, M. Terrazas-López, A. Martínez-Martínez, Á.G. Díaz-Sánchez, FDA-approved thiol-reacting drugs that potentially bind into the SARS-CoV-2 main protease, essential for viral replication, J. Biomol. Struct. Dyn. (2020) 1–9, doi:10.1080/07391102.2020.1764393.
[52] P. Gjerden, L. Slørdal, J.G. Bramness, The use of antipsychotic and anticholinergic antiparkinson drugs in Norway after the withdrawal of orphenadrine, Br. J. Clin. Pharmacol. 68 (2009) 238–242, doi:10.1111/j.1365-2125.2009.03446.x.
[53] M.H. Cheng, E. Block, F. Hu, M.C. Cobanoglu, A. Sorkin, I. Bahar, Insights into the modulation of dopamine transporter function by amphetamine, orphenadrine and cocaine binding, Front. Neurol. 6 (2015), doi:10.3389/fneur.2015.00134.
[54] M.A. El-Nakeeb, H.M. Abou-Shleib, A.M. Khalil, H.G. Omar, O.M. El-Halfawy, In vitro antibacterial activity of some antihistaminics belonging to different groups against Multi-Drug resistant clinical isolates, Brazilian J. Microbiol. 42 (2011) 980–991 /pmc/articles/PMC3768775/?report=abstract (accessed July 9, 2020).
[55] H.S. Maji, S. Maji, M. Bhattacharya, An exploratory study on the antimicrobial activity of cetirizine dihydrochloride, Indian J. Pharm. Sci. 79 (2017) 751–757, doi:10.4172/pharmaceutical-sciences.1000288.
[56] G.G. Bruer, P. Hagedorn, M. Kietzmann, A.F. Tohamy, V. Filor, E. Schultz, S. Mielke-Kuschow, J. Meissner, Histamine H 1 receptor antagonists enhance the efficacy of antibacterials against Escherichia coli, BMC Vet. Res. 15 (2019), doi:10.1186/s12917-019-1797-9.
[57] M. Lagadinou, M.O. Onisor, A. Rigas, D.-V. Musetescu, D. Gkentzi, S.F. Assimakopoulos, G. Panos, M. Marangos, Antimicrobial properties on non-antibiotic drugs in the era of increased bacterial resistance, Antibiotics 9 (2020) 107, doi:10.3390/antibiotics9030107.
[58] O. Trott, A.J. Olson, AutoDock Vina: improving the speed and accuracy of docking with a new scoring function, efficient optimization, and multithreading, J. Comput. Chem. 31 (2010) 455–461, doi:10.1002/jcc.21334.
[59] E.F. Pettersen, T.D. Goddard, C.C. Huang, G.S. Couch, D.M. Greenblatt, E.C. Meng, T.E. Ferrin, UCSF Chimera?A visualization system for exploratory research and analysis, J. Comput. Chem. 25 (2004) 1605–1612, doi:10.1002/jcc.20084.
[60] R.A. Laskowski, M.B. Swindells, LigPlot+: multiple ligand–protein interaction diagrams for drug discovery, J. Chem. Inf. Model. 51 (2011) 2778–2786, doi:10.1021/ci200227u.
[61] J.R. Lakowicz, J.R. Lakowicz, Quenching of fluorescence, in: Principles of Fluorescence Spectroscopy, Springer, US, 1999, pp. 237–265, doi:10.1007/978-1-4757-3061-6_8.
[62] A.I. Martinez-Gonzalez, Á.G. Díaz-Sánchez, L.A. de la Rosa, I. Bustos-Jaimes, E. Alvarez-Parrilla, Inhibition of α-amylase by flavonoids: structure activity relationship (SAR), Spectrochim. Acta Part A Mol. Biomol. Spectrosc. 206 (2019) 437–447, doi:10.1016/j.saa.2018.08.057.
[63] K. Huynh, C.L. Partch, Analysis of protein stability and ligand interactions by thermal shift assay, Curr. Protoc. Protein Sci. (2015), doi:10.1002/0471140864.ps2809s79.
[64] A.J. Miles, B.A. Wallace, Biopharmaceutical applications of protein characterisation by circular dichroism spectroscopy, Biophys. Charact. Proteins Dev. Biopharm. (2020) 123–152, doi:10.1016/B978-0-444-64173-1.00006-8.
[65] N.K. Bari, G. Kumar, J.P. Hazra, S. Kaur, S. Sinha, Functional protein shells fabricated from the self-assembling protein sheets of prokaryotic organelles, J. Mater. Chem. B. 8 (2020) 523–533, doi:10.1039/c9tb02224d.
[66] P. Nath, K. Sharma, K. Kumar, A. Goyal, Combined SAXS and computational approaches for structure determination and binding characteristics of Chimera (CtGH1-L1-CtGH5-F194A) generated by assembling β-glucosidase (CtGH1) and a mutant endoglucanase (CtGH5-F194A) from Clostridium thermocellum, Int. J. Biol. Macromol. 148 (2020) 364–377, doi:10.1016/j.ijbiomac.2020.01.116.
[67] C. Louis-Jeune, M.A. Andrade-Navarro, C. Perez-Iratxeta, Prediction of protein secondary structure from circular dichroism using theoretically derived spectra, Proteins Struct. Funct. Bioinform. 80 (2012) 374–381, doi:10.1002/prot.23188.
[68] L. Sawle, K. Ghosh, How do thermophilic proteins and proteomes withstand high temperature? Biophys. J. 101 (2011) 217–227, doi:10.1016/j.bpj.2011.05.059.
[69] S. Martínez-Caballero, P. Cano-Sánchez, I. Mares-Mejía, A.G. Díaz-Sánchez, M.L. Macías-Rubalcava, J.A. Hermoso, A. Rodríguez-Romero, Comparative study of two GH19 chitinase-like proteins from Hevea brasiliensis, one exhibiting a novel carbohydrate-binding domain, FEBS J. 281 (2014) 4535–4554, doi:10.1111/febs.12962.
[70] R. Cabrera, J. Rocha, V. Flores, L. Vázquez-Moreno, G. Guarneros, G. Olmedo, A. Rodríguez-Romero, M. de la Torre, Regulation of sporulation initiation by NprR and its signaling peptide NprRB: molecular recognition and conformational changes, Appl. Microbiol. Biotechnol. 98 (2014) 9399–9412, doi:10.1007/s00253-014-6094-8.
[71] F. Rasoulzadeh, D. Asgari, A. Naseri, M.R. Rashidi, Spectroscopic studies on the interaction between erlotinib hydrochloride and bovine serum albumin, DARU, J. Pharm. Sci. 18 (2010) 179–184 https://www.ncbi.nlm.nih.gov/pmc/articles/pmid/22615615/?tool=EBI. (accessed July 7, 2020).
[72] E.G. Matveeva, C. Morisseau, M.H. Goodrow, C. Mullin, B.D. Hammock, Tryptophan fluorescence quenching by enzyme inhibitors as a tool for enzyme active site structure investigation: epoxide hydrolase, Curr. Pharm. Biotechnol. 10 (2009) 589–599, doi:10.2174/138920109789069260.
[73] N. Bai, H. Roder, A. Dickson, J. Karanicolas, Isothermal analysis of thermofluor data can readily provide quantitative binding affinities, Sci. Rep. 9 (2019) 1–15, doi:10.1038/s41598-018-37072-x.
[74] R. Velasco-García, V.J. Zaldívar-Machorro, C. Mújica-Jiménez, L. González-Segura, R.A. Muñoz-Clares, Disulfiram irreversibly aggregates betaine aldehyde dehydrogenase—a potential target for antimicrobial agents against Pseudomonas aeruginosa, Biochem. Biophys. Res. Commun. 341 (2006) 408–415, doi:10.1016/j.bbrc.2006.01.003.
[75] C.H. Douse, N. Vrielink, Z. Wenlin, E. Cota, E.W. Tate, Targeting a dynamic protein-protein interaction: fragment screening against the malaria Myosin A motor complex, ChemMedChem 10 (2015) 134–143, doi:10.1002/cmdc.201402357.
[76] A. Kabir, R.P. Honda, Y.O. Kamatari, S. Endo, M. Fukuoka, K. Kuwata, Effects of ligand binding on the stability of aldo-keto reductases: Implications for stabilizer or destabilizer chaperones, Protein Sci. 25 (2016) 2132–2141, doi:10.1002/pro.3036.
[77] P. Cimmperman, L. Baranauskiene, S. Jachimovičiute, J. Jachno, J. Torresan, V. Michailoviene, J. Matuliene, J. Sereikaite, V. Bumelis, D. Matulis, A quantitative model of thermal stabilization and destabilization of proteins by ligands, Biophys. J. 95 (2008) 3222–3231, doi:10.1529/biophysj.108.134973.
[78] A.S. Mahadevi, G.N. Sastry, Cation$-\pi$ interaction: its role and relevance in chemistry, biology, and material science, Chem. Rev. 113 (2013) 2100–2138, doi:10.1021/cr300222d.
[79] T.V. Pyrkov, D.V. Pyrkova, E.D. Balitskaya, R.G. Efremov, The Role of Stacking Interactions in Complexes of Proteins with Adenine and Guanine Fragments of Ligands, Acta Naturae 1 (2009) 124–127, doi:10.32607/20758251-2009-1-1-124-127.
[80] D.D. Boehr, A.R. Farley, G.D. Wright, J.R. Cox, Analysis of the π-π stacking interactions between the aminoglycoside antibiotic kinase APH(3′)-IIIa and its nucleotide ligands, Chem. Biol. 9 (2002) 1209–1217, doi:10.1016/S1074-5521(02)00245-4.
[81] R. Efremov, A. Chugunov, T. Pyrkov, J. Priestle, A. Arseniev, E. Jacoby, Molecular lipophilicity in protein modeling and drug design, Curr. Med. Chem. 14 (2007) 393–415, doi:10.2174/092986707779941050.
[82] A.M. Gallina, P. Bork, D. Bordo, Structural analysis of protein-ligand interactions: the binding of endogenous compounds and of synthetic drugs, J. Mol. Recognit. 27 (2014) 65–72, doi:10.1002/jmr.2332.
[83] D. Dutta, S. Mishra, Structural and mechanistic insight into substrate binding from the conformational dynamics in apo and substrate-bound DapE enzyme, Phys. Chem. Chem. Phys. 18 (2016) 1671–1680, doi:10.1039/C5CP06024A.
[84] G.M. Clore, Interplay between conformational selection and induced fit in multidomain protein-ligand binding probed by paramagnetic relaxation enhancement, Biophys. Chem. 186 (2014) 3–12, doi:10.1016/j.bpc.2013.08.006.
[85] B. Selmke, P.P. Borbat, C. Nickolaus, R. Varadarajan, J.H. Freed, W.E. Trommer, Open and closed form of maltose binding protein in its native and molten globule state as studied by electron paramagnetic resonance spectroscopy, Biochemistry 57 (2018) 5507–5512, doi:10.1021/acs.biochem.8b00322.
[86] R. Bajaj, M.I. Park, C.V. Stauffacher, A.L. Davidson, Conformational dynamics in the binding-protein-independent mutant of the Escherichia coli maltose transporter, MalG511, and its interaction with maltose binding protein, Biochemistry 57 (2018) 3003–3015, doi:10.1021/acs.biochem.8b00266.
[87] J. Badger, J.M. Sauder, J.M. Adams, S. Antonysamy, K. Bain, M.G. Bergseid, S.G. Buchanan, M.D. Buchanan, Y. Batiyenko, J.A. Christopher, S. Emtage, A. Eroshkina, I. Feil, E.B. Furlong, K.S. Gajiwala, X. Gao, D. He, J. Hendle, A. Huber, K. Hoda, P. Kearins, C. Kissinger, B. Laubert, H.A. Lewis, J. Lin, K. Loomis, D. Lorimer, G. Louie, M. Maletic, C.D. Marsh, I. Miller, J. Molinari, H.J. Muller-Dieckmann, J.M. Newman, B.W. Noland, B. Pagarigan, F. Park, T.S. Peat, K.W. Post, S. Radojicic, A. Ramos, R. Romero, M.E. Rutter, W.E. Sanderson, K.D. Schwinn, J. Tresser, J. Winhoven, T.A. Wright, L. Wu, J. Xu, T.J.R. Harris, Structural analysis of a set of proteins resulting from a bacterial genomics project, Proteins Struct. Funct. Bioinform. 60 (2005) 787–796, doi:10.1002/prot.20541.

[88] T.S. Girish, B. Gopal, Crystal structure of Staphylococcus aureus metallopeptidase (Sapep) reveals large domain motions between the manganese-bound and apo-states., J. Biol. Chem. 285 (2010) 29406–29415, doi:10.1074/jbc.M110.147579.
[89] B. Nocek, A. Joachimiak, W.F. Anderson, 1.30 A crystal structure of DapE enzyme from Neisseria meningitidis MC58, 2017. doi:10.2210/pdb5UEJ/pdb.
[90] Crystal structure of a M20A metallo peptidase (dapE, lpg0809) from Legionella pneumophila subsp. pneumophila str. philadelphia 1 at 1.50 a resolution, 2010. doi:10.2210/pdb3PFE/pdb.
[91] A.T. Brunger, D. Das, A.M. Deacon, J. Grant, T.C. Terwilliger, R.J. Read, P.D. Adams, M. Levitt, G.F. Schröder, Application of DEN refinement and automated model building to a difficult case of molecular-replacement phasing: the structure of a putative succinyl-diaminopimelate desuccinylase from corynebacterium glutamicum, Acta Crystallogr. Sect. D Biol. Crystallogr. 68 (2012) 391–403, doi:10.1107/S090744491104978X.